

precursors containing simple alkyl esters underwent Michael addition, but the resulting adducts did not cyclize. Perhaps even more remarkable than the condensation that produces **21** is the parallel transformation of **20** with the enone **4** (Fig. 3, entry 1), which forms (–)-6-deoxytetracycline (**6**) in protected form with >20:1 diastereoselectivity, in 81% yield after purification by RP-HPLC (diastereomerically pure, a minor diastereomer, epimeric at C6, was also isolated separately). It appears that additions to **4** and **5** proceed almost exclusively by addition to one face of each enone (the top face as drawn in Fig. 1B), producing C5a stereochemistry corresponding to that of natural tetracyclines, although why this should be the case is not obvious.

Efficient and stereoselective condensations were not restricted to the *o*-toluate anion derived from the D-ring substrate **20**. In all, we prepared six 6-deoxytetracycline variants (Fig. 3). In each case, it was necessary to optimize the specific conditions for *o*-toluate anion generation and trapping. For the synthesis of products **8**, **9**, and **10** (Fig. 3), anion generation was best conducted in situ, in the presence of the enone **4**, either by selective deprotonation (**8**) or by lithium-halogen exchange (**9** and **10**). A number of potentially competing nonproductive reaction sequences might have intervened during in situ anion generation (such as enolization of **4**); the observed efficiencies of the transformations are surprising in light of this. It is also noteworthy that in situ anion generation permits the use of *o*-toluates lacking an *o*-alkoxy substituent (such as used in the synthesis of **8** and **9**), substrates that are known to be problematic from prior studies (35). Also, lithium-halogen exchange reactions of benzylic halides (such as used in the synthesis of **9** and **10**) had previously been considered impracticable (36, 37).

The efficiencies of the synthetic sequences we report have allowed for the preparation of sufficient quantities of each tetracycline analog for antibacterial testing, using standard serial-dilution techniques (in 5- to 20-mg amounts). Minimum inhibitory concentrations (MICs) were determined for each analog in whole-cell antimicrobial assays using five Gram-positive and five Gram-negative organisms (Fig. 3). Thus far, the pentacycline derivative **10** has shown the most promising antibacterial properties, with activity equal to or greater than tetracycline in each of the Gram-positive strains examined, including strains with resistance to tetracycline, methicillin, and vancomycin. Although this finding is noteworthy, it is very likely that antibiotics with even greater potencies and/or improved pharmacological properties will emerge with further exploration of the complex chemical space now made accessible by the versatile synthetic route described.

References and Notes

- C. Walsh, *Antibiotics: Actions, Origins, Resistance* (American Society for Microbiology Press, Washington, DC, 2003).
- S. G. B. Amyes, *Magic Bullets, Lost Horizons: the Rise and Fall of Antibiotics* (Taylor and Francis, New York, 2001).
- M. Leeb, *Nature* **431**, 892 (2004).
- W. R. Strohl, *Metab. Eng.* **3**, 4 (2001).
- D. E. Cane, C. T. Walsh, C. Khosla, *Science* **282**, 63 (1998).
- L. Katz, *Chem. Rev.* **97**, 2557 (1997).
- C. R. Stephens et al., *J. Am. Chem. Soc.* **85**, 2643 (1963).
- M. Nelson, W. Hillen, R. A. Greenwald, Eds., *Tetracyclines in Biology, Chemistry and Medicine* (Birkhauser Verlag, Boston, 2001).
- D. E. Brodersen et al., *Cell* **103**, 1143 (2000).
- M. Pioletti et al., *EMBO J.* **20**, 1829 (2001).
- P.-E. Sum, P. Petersen, *Bioorg. Med. Chem. Lett.* **9**, 1459 (1999).
- K. Bush, M. Macielag, M. Weidner-Wells, *Curr. Opin. Microbiol.* **7**, 466 (2004).
- J. J. Korst et al., *J. Am. Chem. Soc.* **90**, 439 (1968).
- A. I. Gurevich et al., *Tetrahedron Lett.* **8**, 131 (1967).
- H. Muxfeldt et al., *J. Am. Chem. Soc.* **101**, 689 (1979).
- K. Tatsuta, T. Yoshimoto, H. Gunji, Y. Okado, M. Takahashi, *Chem. Lett. (Jpn.)* **2000**, 646 (2000).
- G. Stork, J. J. La Clair, P. Spargo, R. P. Nargund, N. Totah, *J. Am. Chem. Soc.* **118**, 5304 (1996).
- W. Rogalski, in *Handbook of Experimental Pharmacology*, J. J. Hlavka, J. H. Boothe, Eds. (Springer-Verlag, New York, 1985), vol. 78, chap. 5.
- A. M. Reiner, G. D. Hegeman, *Biochemistry* **10**, 2530 (1971).
- A. G. Myers, D. R. Siegel, D. J. Buzard, M. G. Charest, *Org. Lett.* **3**, 2923 (2001).
- G. Stork, A. A. Hagedorn III, *J. Am. Chem. Soc.* **100**, 3609 (1978).
- D. M. Vyas, Y. Chiang, T. W. Doyle, *Tetrahedron Lett.* **25**, 487 (1984).
- P. Pevarello, M. Varasi, *Synth. Commun.* **22**, 1939 (1992).
- S. H. Pine, *Org. React.* **18**, 403 (1970).
- A. G. Myers, B. Zheng, *Tetrahedron Lett.* **37**, 4841 (1996).
- M. Frigerio, M. Santagostino, *Tetrahedron Lett.* **35**, 8019 (1994).
- E. J. Corey, H. Cho, C. Rucker, D. H. Hua, *Tetrahedron Lett.* **22**, 3455 (1981).
- F. A. Davis, M. C. Weismiller, C. K. Murphy, R. T. Reddy, B.-C. Chen, *J. Org. Chem.* **57**, 7274 (1992).
- E. N. Prilezhaeva, *Russ. Chem. Rev.* **70**, 897 (2001).
- T.-L. Ho, *Tandem Organic Reactions* (Wiley, New York, 1992).
- F. J. Leeper, J. Staunton, *J. Chem. Soc. Chem. Comm.* **1978**, 406 (1978).
- F. M. Hauser, R. P. Rhee, *J. Org. Chem.* **43**, 178 (1978).
- J. H. Dodd, S. M. Weinreb, *Tetrahedron Lett.* **20**, 3593 (1979).
- J. D. White, E. G. Nolen Jr., C. H. Miller, *J. Org. Chem.* **51**, 1150 (1986).
- F. M. Hauser, R. P. Rhee, S. Prasanna, S. M. Weinreb, J. H. Dodd, *Synthesis (Mass.)* **1980**, 72 (1980).
- W. E. Parham, L. D. Jones, Y. A. Sayed, *J. Org. Chem.* **41**, 1184 (1976).
- S. C. Berk, M. C. P. Yeh, N. Jeong, P. Knochel, *Organometallics* **9**, 3053 (1990).
- We thank D. Kahne and C. Walsh for helpful discussions and W. Brubaker (Farmington Pharma Development) and C. Thoma and J. Thanassi (Achillion Pharmaceuticals) for antibacterial screening. This work was supported by NIH grant AI48825, NSF predoctoral graduate fellowships (M.G.C. and J.D.B.), and the Deutscher Akademischer Austausch Dienst (C.D.L.). A.G.M. serves on the scientific advisory boards of Vicuron Pharmaceuticals and Miikana Therapeutics and is a consultant for Pfizer. The research described here is independent.

Supporting Online Material

www.sciencemag.org/cgi/content/full/308/5720/395/DC1

Materials and Methods

References

13 January 2005; accepted 1 March 2005

10.1126/science.1109755

Hypoxia, Global Warming, and Terrestrial Late Permian Extinctions

Raymond B. Huey* and Peter D. Ward

A catastrophic extinction occurred at the end of the Permian Period. However, baseline extinction rates appear to have been elevated even before the final catastrophe, suggesting sustained environmental degradation. For terrestrial vertebrates during the Late Permian, the combination of a drop in atmospheric oxygen plus climate warming would have induced hypoxic stress and consequently compressed altitudinal ranges to near sea level. Our simulations suggest that the magnitude of altitudinal compression would have forced extinctions by reducing habitat diversity, fragmenting and isolating populations, and inducing a species-area effect. It also might have delayed ecosystem recovery after the mass extinction.

A catastrophic extinction marks the end of the Permian (1, 2) and is attributed to an acute climate crisis, among other causes (3–5). However, background extinction rates and ecosystem turnover were elevated throughout much of the Late Permian (6, 7), and recovery after extinction was slow (1, 2). Thus, environmental degradation likely occurred both before and after the final catastrophe, perhaps caused by major shifts in atmospheric chemistry (8). Indeed, modeling, isotope, and

paleontological evidence (9–13) suggests that O₂ levels plummeted in the Late Permian and Early Triassic (Fig. 1A) and would have restricted the supply of O₂ to organisms. At the same time, CO₂ levels were rising (Fig. 1A), and climate warming (14) would have increased metabolic demand for O₂. Severe hypoxia was inevitable (9, 15, 16).

Here, we explore a biogeographic consequence of presumed low O₂ levels during the Late Permian and Triassic: Terrestrial animals

would have been restricted to low altitude, because even moderate altitudes would have insufficient O₂. We simulate the magnitude of altitudinal compression and evaluate its contributions to the high background extinction rate, the catastrophic extinction, and the delayed recovery (1, 2).

Terrestrial animals attempting to live at moderate to high altitude are physiologically challenged by declining temperatures, food supply, habitat area, and O₂ levels, along with increased respiratory water loss (17). The upper altitudinal limits of species likely reflect the influence of these factors as well as ecological, geological, and biogeographic factors (18).

The relative contribution of O₂ in limiting altitudinal ranges has no doubt changed over time because O₂ levels fluctuated so drastically (Fig. 1A). For example, when O₂ levels appear to have been at their zenith during the cold Early Permian [\sim 300 million years ago (Ma), Fig. 1A], the partial pressure of inspired O₂ (P_{IO₂}) even at an altitude of 6 km may have matched that at sea level in today's atmosphere (19). In this glaciated and O₂-rich environment, altitudinal ranges would have been constrained by extreme cold or ice, not by O₂ levels. But when O₂ levels are calculated to be at their nadir during the hot Early Triassic (\sim 240 and \sim 200 Ma), P_{IO₂} even at sea level may have been equivalent to that at \geq 5.3 km in today's atmosphere (Fig. 1B). If estimates of O₂ (Fig. 1A) and climate are correct, the combination of low P_{IO₂} and high temperature would have induced hypoxia and restricted terrestrial vertebrates to low altitudes.

We simulated the impact of O₂ levels on maximum altitudinal ranges of vertebrates having a presumed mid-Permian physiology (20). The actual hypoxia tolerance of mid-Permian ectotherms is of course unknown but was probably lower than that of present-day vertebrates. Mid-Permian vertebrates not only had primitive respiratory systems (9) but also had been evolving in an O₂-rich atmosphere for millions of years (Fig. 1A) and could not have become adapted to altitude (hence, to low O₂ levels) because of icehouse temperatures during that time.

We start by deriving a reference set of hypothetical species living in the mid-Permian and having maximum altitudes ranging from 2.0 to 8.0 km, in 1-km intervals. We assume that the maximum altitude of each species was set by—or at least strongly influenced by—the critical P_{IO₂} occurring at that altitude. Then, assuming that hypoxia tolerances were constant over time (i.e., always had the same critical P_{IO₂}), we calculate how maximum

altitudes (Fig. 1C) changed with O₂ levels (Fig. 1A). This involves estimating the average P_{IO₂} at each altitude during the mid-Permian and then computing (at intervals of 10 million years) the altitude where each P_{IO₂} would have occurred (20).

The presumed drop in O₂ levels during the Late Permian (Fig. 1A) would have drastically compressed the altitudinal ranges of all hypothetical species (Fig. 1C). If O₂ levels dropped to \sim 16% at the end of the Permian (8), P_{IO₂} at sea level would have been equivalent to that found today at 2.7 km. Animals with limited hypoxia tolerance would have gone extinct (Fig. 1C). To survive, a species would have needed to tolerate a P_{IO₂} at least equivalent to that found at 6.0 km (red line, Fig. 1C) in the mid-Permian (21, 22).

O₂ levels are thought to have continued to drop into the Early Triassic and to have stayed relatively low for the next 100 million years

(Fig. 1A). In addition, CO₂ levels (Fig. 1A) and global temperatures (14) remained high. Thus, hypoxia and the resultant altitudinal compression likely persisted into the early Cretaceous (Fig. 1, A and C) and may have contributed to a slow recovery after the mass extinction (1, 2).

Our simulations (Fig. 1, B and C) focus on O₂ levels, but rising temperatures in the Late Permian and Early Triassic (14) would have exacerbated hypoxia. To reduce the impact, ectotherms could have dispersed along sea-level corridors to high latitudes, thereby lowering their body temperatures. Alternatively, they could have invaded relatively cool aquatic habitats. Indeed, air-breathing aquatic reptiles (e.g., ichthyosaurs, phytosaurs) diversified at this time.

Freshwater-breathing ectotherms were also probably restricted to low altitudes during O₂ lows. Reduced atmospheric O₂ levels

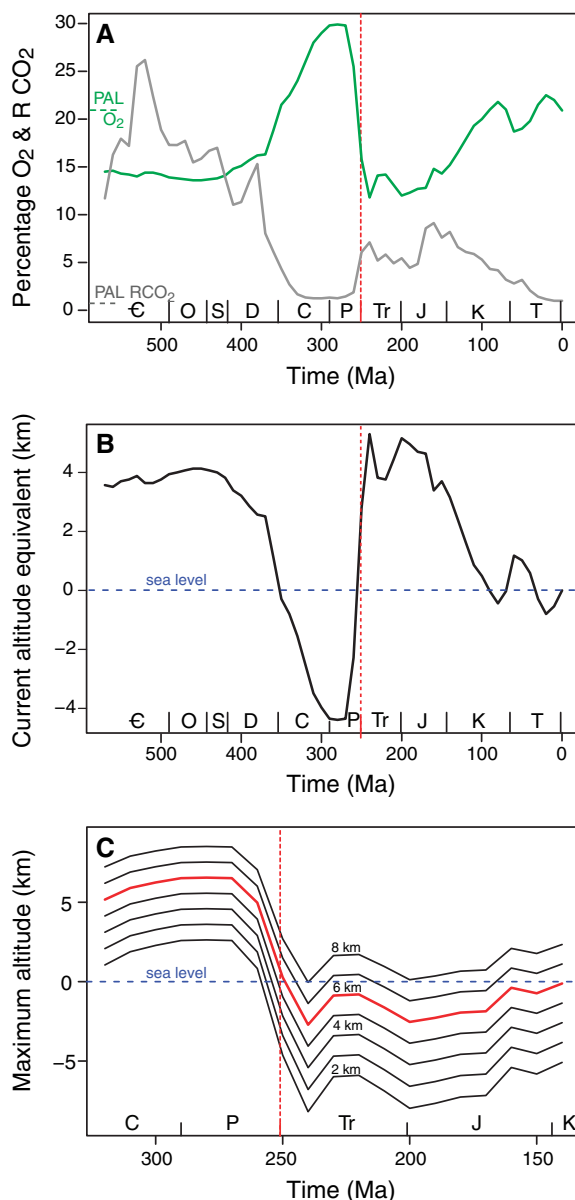


Fig. 1. (A) Percent O₂ over time (green) and the concentration of CO₂ (gray) relative to present-day level (PAL) of each gas is indicated. Global hypoxia would have occurred in the Late Permian and Triassic because of dropping O₂ combined with rising temperatures [data from (4, 37)]. The mass extinction at the Permian-Triassic boundary is indicated by a red dashed line. (B) Present-day altitude with P_{IO₂} equivalent to that at sea level in the Phanerozoic. Thus, P_{IO₂} at sea level at the Triassic O₂ minimum would be found today at \sim 5 km. (C) Predicted maximum altitude over time for hypothetical species having graded tolerances (2 to 8 km) to hypoxia. From the Late Permian through the Jurassic, however, P_{IO₂} was sufficiently low that ranges would have been compressed to near sea level, and some species would have gone extinct. Period codes: C, Cambrian; O, Ordovician; S, Silurian; D, Devonian; C, Carboniferous; P, Permian; Tr, Triassic; J, Jurassic; K, Cretaceous; T, Tertiary.

Department of Biology, University of Washington, Box 351800, Seattle, WA 98195, USA.

*To whom correspondence should be addressed. E-mail: hueyrb@u.washington.edu

plus warm water temperatures would lower aquatic O₂ levels, but warm body temperatures increase O₂ demand. Thus, water-breathing ectotherms would likely have been O₂ challenged, even near sea level.

Insects, which suffered major extinctions during the Late Permian (23), might also have experienced some hypoxia and altitudinal compression. Insect development is slowed by low PO₂ plus warm temperatures (24). Interestingly, giant dragonflies, which evolved during the Permian O₂ high, are thought to have gone extinct in the Late Permian because of limitations on O₂ diffusion (9). However, today's large adult insects rely on convective ventilation and are remarkably hypoxia tolerant (25); thus, the aquatic larvae of giant insects may have been the primary targets of hypoxia-induced extinction.

Altitudinal compression would have had important biogeographic consequences. Animals specialized for upland habitats could not have survived, as they would have been physiologically excluded from them. Moreover, mountain passes would have seemed physiologically higher to animals (26) than are passes of equivalent altitude today. Thus, populations would have become fragmented and isolated (fig. S2), and rates of local extinction may have increased (27).

Altitudinal compression plus rising sea levels at the very end of the Permian (14, 28) would have also reduced the land surface physiologically accessible to animals. This loss would have caused additional extinctions via a species-area effect (29) and also would have delayed the recovery.

Topographic maps for the mid-Permian to Late Permian (30) enable us to estimate (20), albeit with substantial uncertainty, the percentage of the land surface that was physiologically accessible to animals with specified hypoxia tolerance (Fig. 2). During the O₂ high in the Permian, virtually the entire surface of Earth had sufficient O₂ to sustain populations of our hypothetical species. By the Triassic, however, hypoxia would have reduced acces-

sible land area for all but the most hypoxia-tolerant species (Fig. 1C). For example, a species physiologically capable of surviving up to 6.0 km in the mid-Permian would have been restricted to below 0.3 km by the Triassic; thus, it would have been excluded from more than half of the available land surface (gray dotted line in Fig. 2). By the early Triassic (Fig. 1A), even a species that could tolerate 8.0 km in the mid-Permian would have likely gone extinct (Fig. 1C) in the absence of compensatory adaptation. Thus, altitudinal compression could have had substantial effects on extinction and recovery rates, given the huge loss in land for all but the most hypoxia-resistant taxa (Fig. 2).

The reasonableness of our scenario of hypoxia-induced altitudinal compression depends fundamentally on the accuracy and timing of estimates of percent O₂ (8). Those estimates, of course, have uncertainty (8, 20), and other models can yield somewhat different estimates (12, 13).

Our analyses also assume that O₂ restricted the upper altitudinal limits during the Late Permian and Triassic, that terrestrial vertebrates then had modest hypoxia tolerance, and that adaptation to hypoxia was limited. None of these assumptions can be directly tested as yet, but our compression hypothesis leads to predictions and patterns that are subject to test:

1) Terrestrial vertebrates that did survive the Late Permian should show respiratory adaptations for hypoxia. Indeed, morphological traits of *Lyostrosaurus*, one of the few surviving therapsids, and of other Triassic dicynodonts have been interpreted as adaptations to hypoxia (16, 31).

2) Hyperventilation in response to hypoxia would have elevated respiratory water loss during the Late Permian. Maxilloturbinate, which reduce respiratory water loss, first evolved at that time in mammal-like reptiles (32). Turbinates have been interpreted as indicating high respiratory rates associated with endothermy (32), but they might also be

indicators of high respiratory rates induced by hypoxia.

3) Fossil sites for terrestrial ectotherms by the Triassic should be located predominantly at high latitude, where relatively cooler temperatures would reduce metabolic requirements for O₂ and ameliorate hypoxia. Distributional data for therapsids are consistent (33). However, therapsids might also have been restricted to high latitude simply because low-latitude sites were hot, dry, and had a depauperate flora (34).

4) The compression-forced isolation of taxa into refugia could help to explain Late Permian endemism (33), which is surprising for a Pangaeon supercontinent. It could also help to explain the "Lazarus effect" (i.e., the reappearance of taxa that disappeared from the fossil record) noted in this period (1, 35).

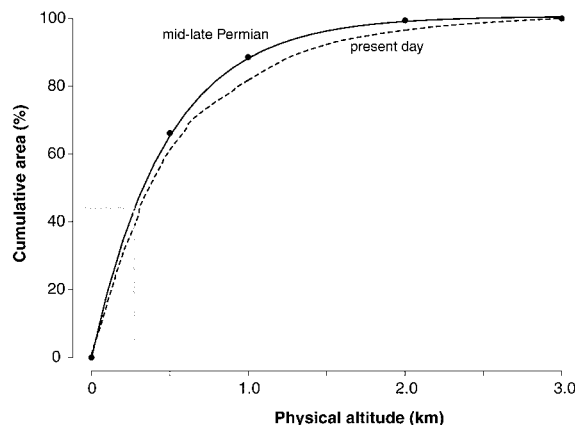
The extinctions during the Late Permian were the largest ever during the history of life on Earth. An abrupt climate change is thought to be responsible for the catastrophic extinction. Nonetheless, hypoxia may have contributed to the high background extinctions and high faunal turnover occurring before the mass extinction, to the final catastrophe itself, and to the delayed recovery. Low O₂ levels would have promoted extinction and delayed recovery directly via physiological stress (16) and indirectly via altitudinal compression.

Note added in proof: A forthcoming paper (36) provides new and fine-scaled estimates of O₂ levels during the Late Permian and Early Triassic. The drop in O₂ during the Late Permian is slightly more recent than that in Fig. 1A, but still suggests that hypoxia and altitudinal compression were influential both before and after the mass extinction.

References and Notes

1. D. H. Erwin, *The Great Paleozoic Crisis* (Columbia Univ. Press, New York, 1993).
2. S. A. Bowring, D. H. Erwin, Y. Isozaki, *Proc. Natl. Acad. Sci. U.S.A.* **96**, 8827 (1999).
3. A. H. Knoll, R. K. Bambach, D. E. Canfield, J. P. Grotzinger, *Science* **273**, 452 (1996).
4. R. A. Berner, *Proc. Natl. Acad. Sci. U.S.A.* **99**, 4172 (2002).
5. M. J. Benton, R. J. Twitchett, *Trends Ecol. Evol.* **18**, 358 (2003).
6. M. J. Benton, V. P. Tverdokhlebov, M. V. Surkov, *Nature* **432**, 97 (2004).
7. P. D. Ward et al., *Science* **307**, 709 (2005); published online 20 January 2005 (10.1126/science.1107068).
8. R. A. Berner, *Geochim. Cosmochim. Acta* **65**, 685 (2001).
9. J. B. Graham, R. Dudley, N. Aguilar, C. Gans, *Nature* **375**, 117 (1995).
10. A. C. Lasaga, H. Ohmoto, *Geochim. Cosmochim. Acta* **66**, 361 (2002).
11. N. D. Sheldon, G. J. Retallack, *Geology* **30**, 919 (2002).
12. N. M. Bergman, T. M. Lenton, A. J. Watson, *Am. J. Sci.* **304**, 397 (2004).
13. R. A. Berner, *The Phanerozoic Carbon Cycle: CO₂ and O₂* (Oxford Univ. Press, Oxford, 2004).
14. D. L. Kidder, T. R. Worsley, *Palaeogeogr. Palaeoclimatol. Palaeoecol.* **203**, 207 (2004).
15. R. A. Berner, D. J. Beerling, R. Dudley, J. M. Robinson, R. A. Wildman Jr., *Annu. Rev. Earth Planet. Sci.* **31**, 105 (2003).
16. G. J. Retallack, R. M. H. Smith, P. D. Ward, *Geol. Soc. Am. Bull.* **115**, 1133 (2003).

Fig. 2. Plot of cumulative land area versus physical altitude during the mid-Permian to Late Permian [solid line (30)] and for the present day [dashed line (20)]. This relationship enables us to estimate the percentage of the land surface that was physiologically tolerable (20) for the hypothetical species shown in Fig. 1C. A species capable of surviving up to 6.0 km in the mid-Permian would be restricted to below 0.3 km by the end of the Permian (gray dotted line) and thus would have been able to occupy less than half of the available land area. Less hypoxia-tolerant species would have gone extinct; more tolerant ones would have suffered minimal area loss.



17. P. Bouverot, *Adaptation to Altitude-Hypoxia in Vertebrates* (Springer-Verlag, Berlin, 1985).
18. K. J. Gaston, *The Structure and Dynamics of Geographic Ranges* (Oxford Univ. Press, Oxford, 2003).
19. We estimate PIO_2 rather than PO_2 , because the addition of respiratory water vapor reduces the partial pressure of O_2 in the lung (20).
20. See supporting data on Science Online.
21. Estimates of maximum altitudes for the Late Permian and Triassic are somewhat low because warm temperatures would have elevated barometric pressure at altitude. However, the impact on O_2 would have been small: Substituting PO_2 and temperature estimates in the hypsometric equation demonstrates that our altitudinal estimates for the Triassic O_2 low (Fig. 1C) underestimate actual limits by at most 0.1 km (22). Similarly, our estimates of maximum altitudes in the cold mid-Permian (Fig. 1C) overestimate actual limits by at most ~0.2 km (22). Because these effects are relatively small, we ignore them in our simulations.
22. D. Battisti, personal communication.
23. C. C. Labandeira, J. J. Sepkoski Jr., *Science* **261**, 310 (1993).
24. M. R. Frazier, H. A. Woods, J. F. Harrison, *Physiol. Biochem. Zool.* **74**, 641 (2001).
25. K. J. Greenlee, J. F. Harrison, *J. Exp. Biol.* **207**, 497 (2004).
26. D. H. Janzen, *Am. Nat.* **101**, 233 (1967).
27. I. A. Hanski, *Metapopulation Ecology* (Oxford Univ. Press, Oxford, 1999).
28. A. Hallam, P. B. Wignall, *Earth Sci. Rev.* **48**, 217 (1999).
29. M. L. Rosenzweig, *Species Diversity in Space and Time* (Cambridge Univ. Press, Cambridge, 1995).
30. D. B. Rowley, R. T. Pierrehumbert, B. S. Currie, *Earth Planet. Sci. Lett.* **88**, 253 (2001).
31. K. Angielczyk, personal communication.
32. W. J. Hillenius, J. A. Ruben, *Physiol. Biochem. Zool.* **77**, 1019 (2004).
33. C. A. Sidor *et al.*, *Nature*, in press.
34. P. M. Rees, *Geology* **30**, 827 (2002).
35. P. B. Wignall, M. J. Benton, *J. Geol. Soc. London* **156**, 453 (1999).
36. R. A. Berner, *Geochim. Cosmochim. Acta*, in press.
37. R. A. Berner, Z. Kothavala, *Am. J. Sci.* **301**, 182 (2001).
38. We thank R. Berner for providing data, advice, and discussion; K. Angielczyk, M. Benton, R. Buick, C. Carey, T. Daniel, R. Dudley, D. Erwin, J. Graham, T. Hornbein, D. Rowley, J. Ruben, A. Smith, M. Stoeck, and J. West for discussion; D. Battisti for computing the impact of temperature on critical altitudes; and D. Rowley and G. Wang for calculating hypsometric data. Supported by NSF grant IBN-0416843 (R.B.H.) and the NASA Astrobiology Institute (University of Washington Node, P.D.W., principal investigator).

Supporting Online Material

www.sciencemag.org/cgi/content/full/308/5720/398/DC1

Materials and Methods

Figs. S1 and S2

References

29 November 2004; accepted 15 February 2005

10.1126/science.1108019

Open-System Coral Ages Reveal Persistent Suborbital Sea-Level Cycles

William G. Thompson*† and Steven L. Goldstein

Sea level is a sensitive index of global climate that has been linked to Earth's orbital variations, with a minimum periodicity of about 21,000 years. Although there is ample evidence for climate oscillations that are too frequent to be explained by orbital forcing, suborbital-frequency sea-level change has been difficult to resolve, primarily because of problems with uranium/thorium coral dating. Here we use a new approach that corrects coral ages for the frequently observed open-system behavior of uranium-series nuclides, substantially improving the resolution of sea-level reconstruction. This curve reveals persistent sea-level oscillations that are too frequent to be explained exclusively by orbital forcing.

The idea that Quaternary climate cycles are linked to changes in Earth's orbit is central to climate change theory (1). The primary evidence for this comes from the marine oxygen isotope ($\delta^{18}O$) record (2) and early dating of coral terraces (3). However, there is abundant evidence for abrupt climate change that was too frequent to be explained by orbital changes (4). Here we attempt to reconstruct sea level between 70 and 240 thousand years ago (ka) with a resolution sufficient to detect suborbital-frequency oscillations, using a new approach to U/Th coral dating (5). Several recent lines of evidence suggest that sea level may be more variable than previously thought. An example is the conversion, via a hydraulic model, of a salinity record from the Red Sea into a sea-level curve for the past 470

thousand years (ky) (6). This record suggests fairly large (~35 m) suborbital-frequency sea-level changes during glacial periods such as marine isotope stage 3 (MIS 3) and more modest (~15 m) changes during interglacials (for example, during MIS 5). This new Red Sea record augments a growing body of evidence for suborbital sea-level fluctuations in coral records. At the Huon Peninsula of Papua New Guinea, multiple coral terraces were formed during MIS 3, with highstands occurring about every 6 ky (7, 8). There are also more Huon terraces associated with MIS 5 than can be accounted for by orbital variability (9). Such evidence is not restricted to New Guinea; closely spaced terraces on Barbados suggest suborbital period changes in sea level during MIS 5a and MIS 5c (9, 10).

The construction of a high-resolution sea-level record requires a large number of accurate coral ages from a limited geographic area, and this has not been possible with standard dating methods. The conventional equations for U/Th age determination (11) require that loss or gain of U and Th have not occurred except by radioactive decay after coral death. This closed-system requirement

is often violated in fossil corals as a result of the alpha-recoil mobility of U-series nuclides (12), and an initial coral $^{234}U/^{238}U$ ratio that is significantly different from that of modern seawater is taken as evidence of open-system behavior and an unreliable age (13). Building on earlier attempts to correct for open-system behavior (14), we have derived a set of decay equations that corrects coral ages for these effects (5). Although conventional U-series coral ages from a single stratigraphic level often differ substantially, open-system ages of these corals are in much better agreement (Fig. 1, A to C), which illustrates the dramatic improvement in the accuracy of coral ages achieved through open-system dating. It has long been known that many conventional coral ages are unreliable, prompting screening for open-system effects (13). Such screening improves accuracy but often results in the rejection of up to 90% of measured ages, degrading the resolution of sea-level reconstructions (fig. S1, A and B). By recovering accurate ages for most corals, the open-system method greatly improves the resolution of the resulting record (fig. S1C).

We have constructed (15) a high-resolution uplift-corrected sea-level curve for Barbados (Fig. 2), with open-system ages calculated from published isotope ratio data (5, 13, 16, 17) and other measurements (table S1). Corals defining this curve are almost entirely *Acropora palmata*, a reef-crest species. An average data density approaching one age per 1000 years during MIS 5 highstands and one age per 2500 years during MIS 7 (to 220 ka) resolves sea-level fluctuations occurring over a few thousand years. For the most part, clearly separated peaks constrained by multiple coral ages define the oscillations characterizing suborbital sea-level variability. However, in mid-MIS 7, between 200 and 220 ka, three potential sea-level peaks are poorly resolved because of overlapping error envelopes. The best constrained portion of the sea-level curve is during MIS 5c, where minor highstands at 100, 103, and 105.5 ka are evident in coral ages from a

Lamont-Doherty Earth Observatory (LDEO) and Department of Earth and Environmental Sciences, Columbia University, Palisades, NY 10964, USA.

*Present address: Department of Geology and Geophysics, 118 Clark Lab, Mail Stop 23, Woods Hole Oceanographic Institution, Woods Hole, MA 02543, USA.

†To whom correspondence should be addressed. E-mail: wthompson@whoi.edu